

FINAL TECHNICAL REPORT
Award Number: G12AP20018

Title: “Improving Regional Ground Motion Attenuation Boundaries and Models Using EarthScope USArray Data for Use in the National Seismic Hazards Mapping Project”

Chris H. Cramer and Md. Nayeem Al Noman
Center for Earthquake Research and Information
University of Memphis
3890 Central Ave
Memphis, TN 38152-3050
901-678-4992
FAX: 901-678-4734
cramer@ceri.memphis.edu

Heather R. DeShon
Huffington Department of Earth Sciences
Southern Methodist University
PO Box 750395
Dallas, TX 75275-0395
214-768-2916
FAX: 214-768-2701
hdeshon@smu.edu

January 1, 2012 – December 31, 2013

Submitted: April 2, 2014

“Research supported by the U.S. Geological Survey (USGS), Department of Interior, under USGS award number G12AP20018. The views and conclusions contained in this document are those of the authors and should not be interpreted as necessarily representing the official policies, either expressed or implied, of the U.S. Government.”

Abstract

EarthScope USArray provides an excellent opportunity to improve the scientific understanding of crustal attenuation in the continental US. Initial work on regional variations in crustal attenuation using USArray has focused on the western US (WUS) (Phillips and Stead, 2008). Efforts have been made to understand regional crustal attenuation outside of the WUS (i.e., Benz et al., 1997; Erickson et al., 2004) but have been limited in scope due to sparse regional seismograph coverage and lower rates of earthquake occurrence in eastern North America (ENA). We focused on data collection and better defining (1) the location and character of Q transitions between major tectonic regions west of the Mississippi River, (2) the regional Q in the Grand Banks and easternmost Canada, and (3) the regional Q in less studied areas of ENA west of the Mississippi River. The “Q” needed is the apparent Q due to the decay of ground motion with distance and not material Q. Q boundary detection was accomplished by using transects of USArray observations across these transitions to look for major changes in regional Q. The three major Q transitions addressed so far have been the WUS-CEUS transition in the Rocky Mountains and Great Plains between 100°W and 115°W, the WUS-Gulf Coast transition in western Texas, and the western portion of the CEUS mid-continental to Gulf Coast transition from Texas to the Mississippi River. Using narrow bandpass filtering and an approach similar to Benz et al. (1997) and Erickson et al. (2004) we determined new regional Q estimates for the Grand Banks / easternmost Canada, the western Gulf Coast, and the Great Plains.

Approach

Q Boundary Detection

We started with selecting the events that have good USArray station coverage in the possible boundary locations in the major tectonic regions of WUS-CEUS and CEUS-Gulf Coast. The emphasis initially is on larger magnitude earthquakes to have good signal to noise over the large distances from the event covered by USArray.

Data processing included data retrieval, instrument correction, and band-pass filtering to a range of frequencies with acceptable signal-to-noise (greater than one). The procedures employed are the same as used in developing the Next Generation Attenuation (NGA) East database of ground motions (Cramer, 2008, and Cramer et al., 2009, 2011). A part of this effort is quality assurance to remove records with data problems and insufficient bandwidth in the 0.1 to 20 Hz range.

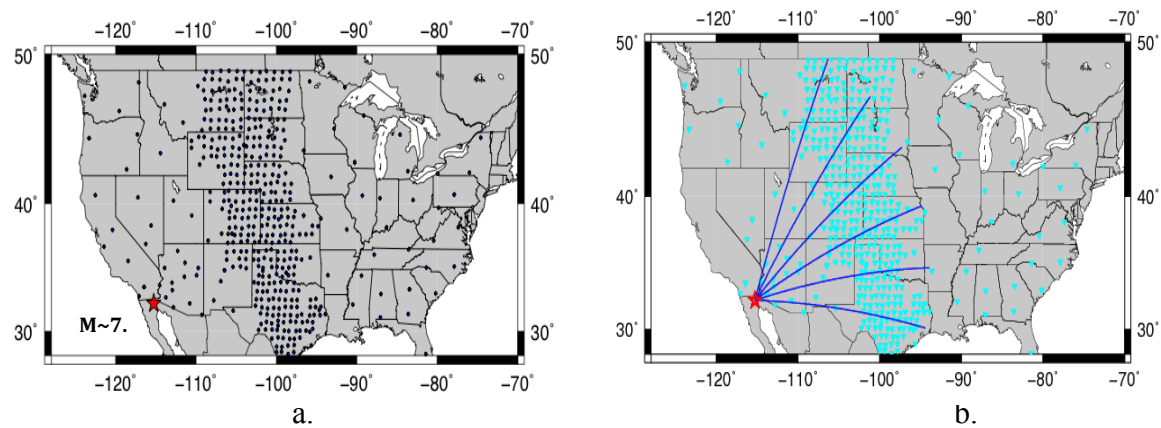


Figure 1: a) Map showing stations for a Baja, California event, b) Map showing transect of profiles from the epicenter.

Figure 1 shows an example for a M7.2 earthquake in Baja California, Mexico. We made transects that extend radially from the epicenter through the TA stations and selected the stations that lay within an azimuth range of 15° along each transect. We then processed the data for peak ground acceleration and velocity, and for spectral acceleration at 0.2 sec and 1.0 sec and plotted the profile of those ground motion records against epicentral distance for our Q boundary transition analysis (Figure 2).

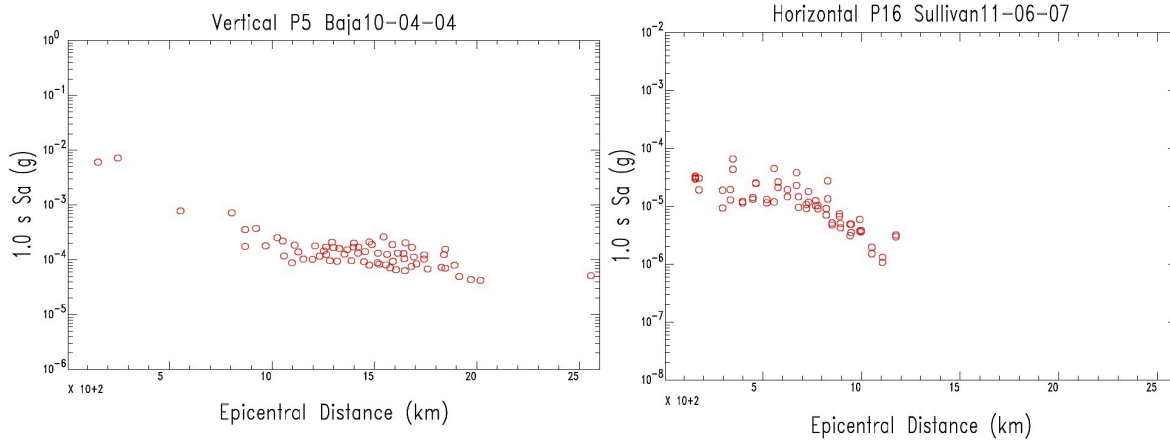


Figure 2: Plot of vertical spectral ground motion for a transect for the M~7.2 Baja, California earthquake (see Figure 1) and Sullivan, Missouri (M~4.2) event at 1.0 sec.

We looked beyond 150 km for any strong change in the slope that is obvious in the ground motion profile. The location of the change the slope gives us a possible estimate of the transition boundary between the tectonic regions. In some cases, due to sparse station coverage, locating the transition in the slope precisely is difficult as shown in Figure 3. However, these transects help constrain the location of the boundary, which might be ultimately found using similar profiles from other suitable events.

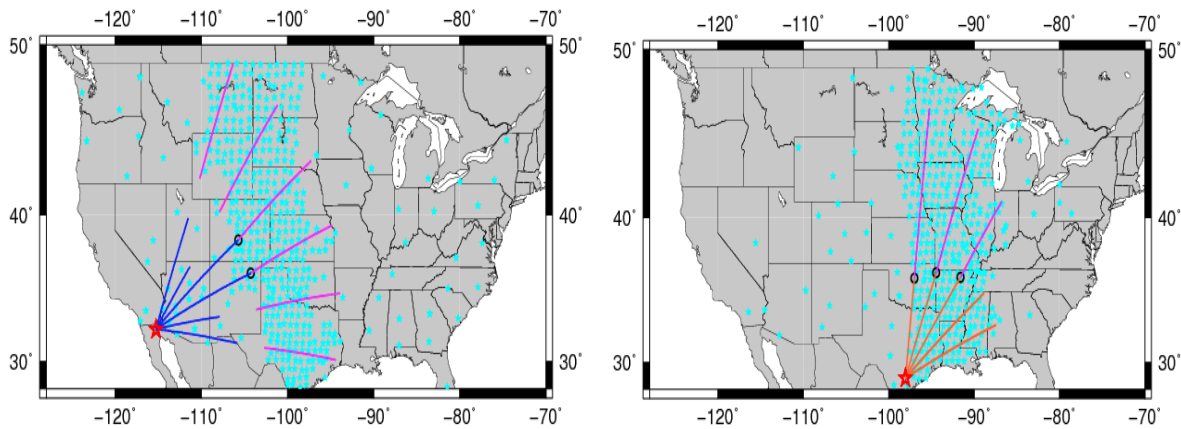


Figure 3: Mapping transition observations from ground motion transects.

Regional Q Estimates

For estimating regional Q we used an approach similar to Benz et al. (1997) and Erickson et al. (2004). Our modification is to use narrow bandpass filtering of velocity records to estimate amplitude at a given frequency at each station for a given earthquake. The four-pole Butterworth narrow bandpass center frequencies (f) used are 1.0, 1.3, 2.0, 3.0, 4.0, 6.0, 8.0, 10.0, 13.0, and 16.0 Hz with filter corners set $0.025 \log(f)$ below and above the center f (log is logarithm base

10). The filtering was accomplished using SAC (Goldstein et al., 2003). We fit observations of amplitudes with distance at a specific frequency to the form

$$\ln(y) = A + C \cdot \text{dist} - 0.5 \cdot \ln(\text{dist}), \quad (1)$$

where y is maximum amplitude at frequency f , dist is epicentral distance, and A and C are constants. \ln is natural logarithm. Geometrical spreading is assumed to be $R^{-0.5}$, which is typical at distances beyond 150 to 200 km in ENA (Atkinson and Mereu, 1992). Q at frequency f can then be determined from

$$Q(f) = -\pi \cdot f / C \cdot \beta, \quad (2)$$

where C is from the fit to Equation 1 at frequency f and β is crustal shear-wave velocity (3.5 km/s from Benz et al., 1997). All the values of Q at different frequencies can then be fit using

$$\log [Q(f)] = \log (Q_0) + \eta \cdot \log(f), \quad (3)$$

where Q_0 is the Q at 1 Hz and η is the power of f in $Q(f) = Q_0 \cdot f^\eta$. Q_0 and η represent the regional Q that can be compared with values from other studies in different regions. All fits are determined by linear least squares inversion (Claerbout, 1976) using the elimination method (Faddeeva, 1959). Regional Q estimates determined in this study are whole record (S and Lg dominate) estimates and are similar to the ENA Q estimate of Atkinson and Boore (2014).

Results

Q Boundary

Table 1 lists the events used in our analysis. Eight more WUS events were examined but had similar source locations to the WUS earthquakes listed or the USArray was not deployed in a useful location, so these events provided no additional information (Table 2).

Table 1: List of earthquakes with usable transects used in the initial analysis.

WUS-CEUS/Gulf Coast

Baja, California 10-04-04 M~7.2
 Nevada 08-02-21 M5.9
 Gulf of California 09-08-05 M~5.8
 Baja, California 09-12-30 M~5.9

Gulf Coast-CEUS

Comal, TX 11-10-20 M4.6
 Sparks, OK 11-11-06 M5.6
 Greenbrier, AR 11-02-28 M4.7
 Sullivan, MO 11-06-07 M3.9
 Mineral, VA 11-08-23 M5.7
 Val des Boise 10-06-23 M5.0

Table 2: List of WUS earthquakes examined but not used in the initial analysis due to redundant and/or inadequate TA array coverage.

Off Oregon Coast 08-01-10 M6.3
 Off S. Oregon Coast 08-03-15 M5.7
 Gulf of California 09-08-03 M6.9
 Los Angeles, CA 08-07-29 M5.5
 Offshore N. California 08-11-28 M5.9
 Offshore N. California 10-01-10 M6.5
 Offshore N. California 10-02-04 M5.9
 Southern California 08-12-06 M5.1

Figure 4 shows our initial map of possible transition locations between the regions. The addition of more suitable events will help sharpen the boundary locations and fill in the gap where we still need information on the transitions. Additionally, a finer azimuthal spacing (reducing to a 5° increment in azimuth) can help provide more detail along some segments of the transition. Figure 4 can also serve as a guide to selecting station-paths for more detailed regional Q determinations using the approach of Benz et al., 1997 and Erickson et al., 2004 and eventually using tomographic inversion for Q.

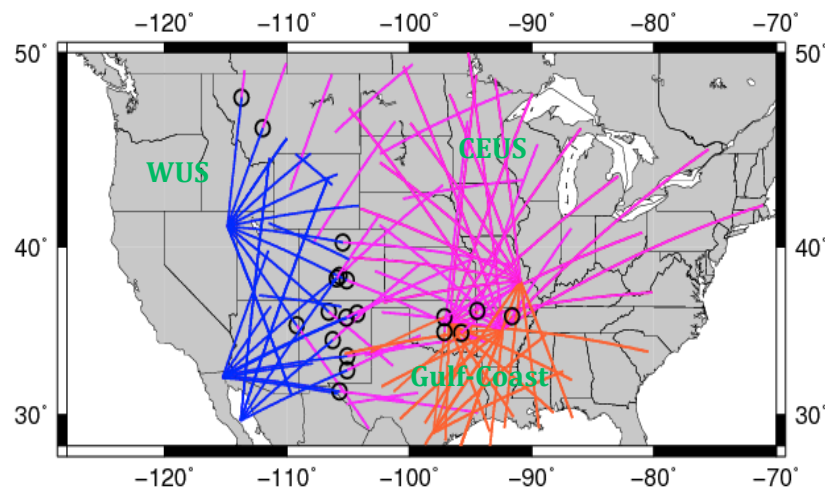


Figure 4: Map showing possible trend of boundary locations.

Regional Q Estimates

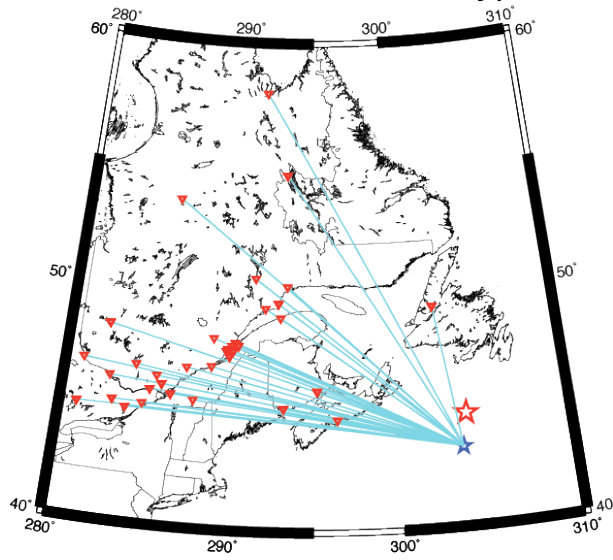
Easternmost Canada: A major focus of our regional Q estimation is easternmost Canada and the offshore Grand Banks area. A better understanding of regional Q is needed for this part of Canada because the 1929 Grand Banks M7.2 earthquake is a key reference event for estimating magnitudes of other historic M7 earthquakes in eastern North America – mainly the 1811-1812 New Madrid and 1886 Charleston earthquakes (Cramer and Boyd, 2014). Table 3 lists earthquakes in this region used in our regional analysis.

Table 3: Easternmost Canada and Grand Banks earthquakes used in this study. Unless otherwise indicated, magnitudes are from the Geological Survey of Canada. The presence or absence of Lg is also indicated.

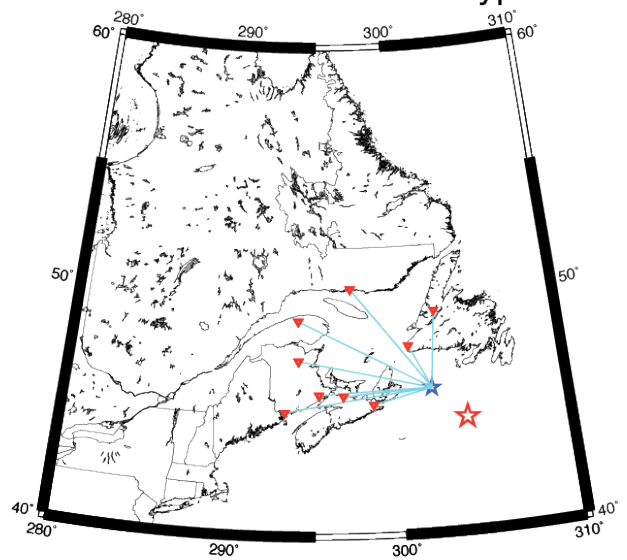
Laurentian Fan 2005/01/25 Mw4.0 (magnitude from Cramer and Boyd, 2014) – No Lg
Laurentian Channel 2006/02/03 m_N3.0 – No Lg
Atlantic Ocean 2007/03/08 M_L4.2 – No Lg
Laurentian Channel 2007/05/30 m_N3.0 – Lg present
Atlantic Ocean 2010/11/05 M_L4.4 – No Lg
Laborador 2012/07/08 Mw4.4 (magnitude from SLU moment tensor catalog) – Lg present
Offshore Newfoundland 2013/03/09 M_L4.3 – Weak Lg

Figure 5 presents raypath coverage for the earthquakes in Table 3. Microseisms limit the earthquake observable frequency band from 1.0 or 2.0 Hz to 10 Hz on many records because of station locations near the Atlantic coast. Figure 6 presents the Q(f) results for each earthquake.

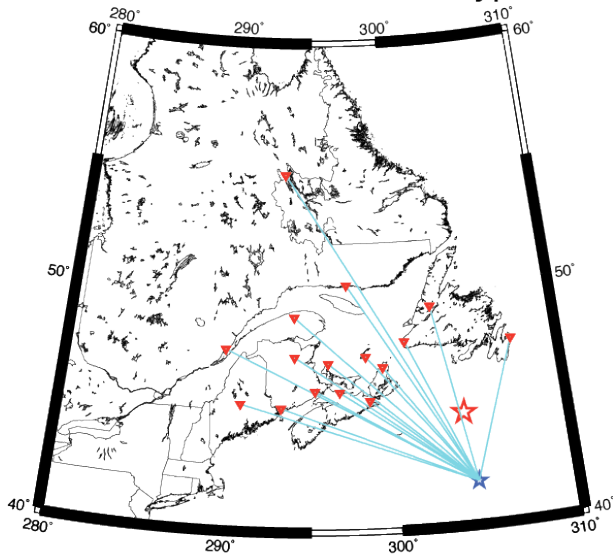
Grand Banks 2005/01 Raypaths



Grand Banks 2006/02 Raypaths



Grand Banks 2007/03 Raypaths



Grand Banks 2007/05 Raypaths

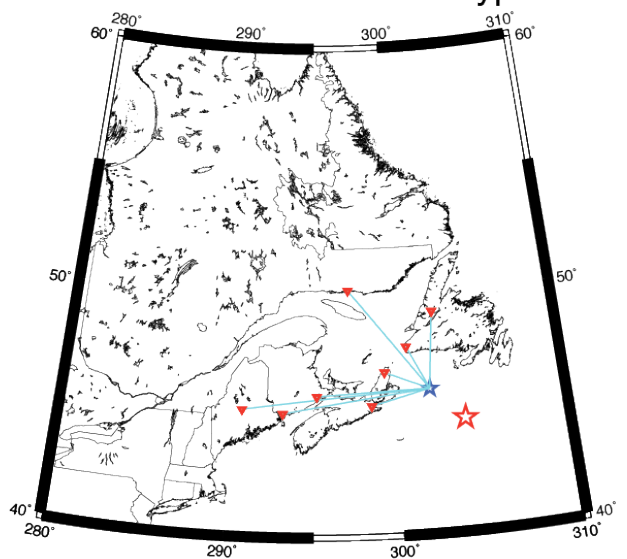
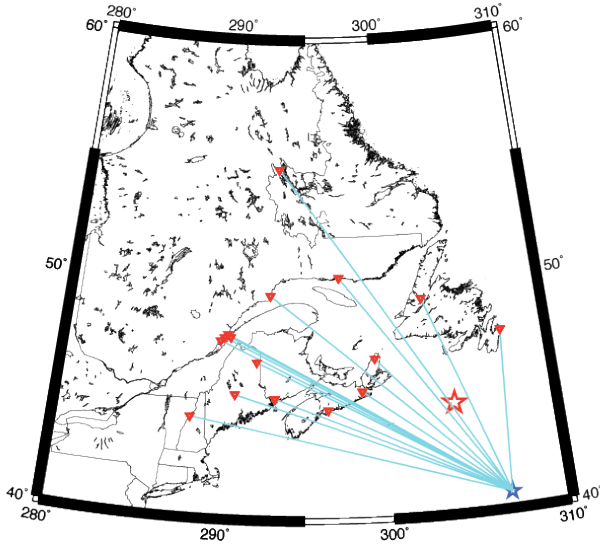
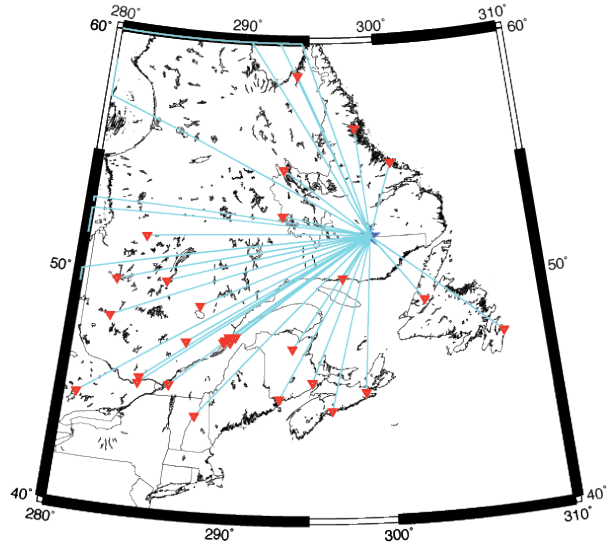


Figure 5: Raypath (light blue) maps for seven easternmost Canada earthquakes (blue star). Red inverted triangles are stations recording each earthquake and the large red star is the location of the 1929 Grand Banks earthquake (Grand Banks events only).

Grand Banks 2010/11 Raypaths



Labrador 2012/07 Raypaths



E of Newfoundland 2013/03 Raypaths

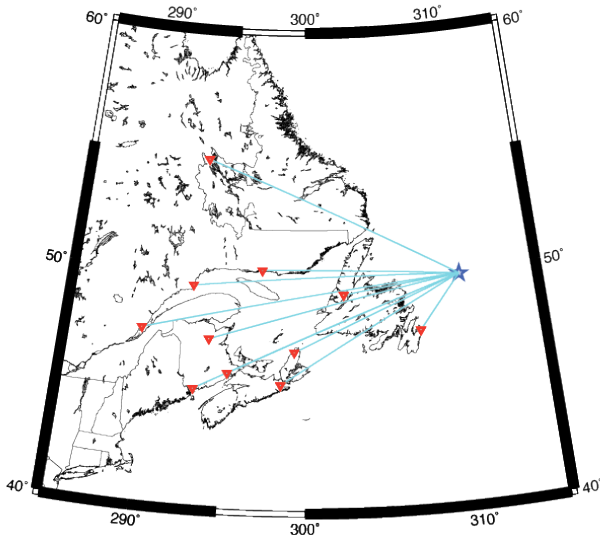


Figure 5 continued.

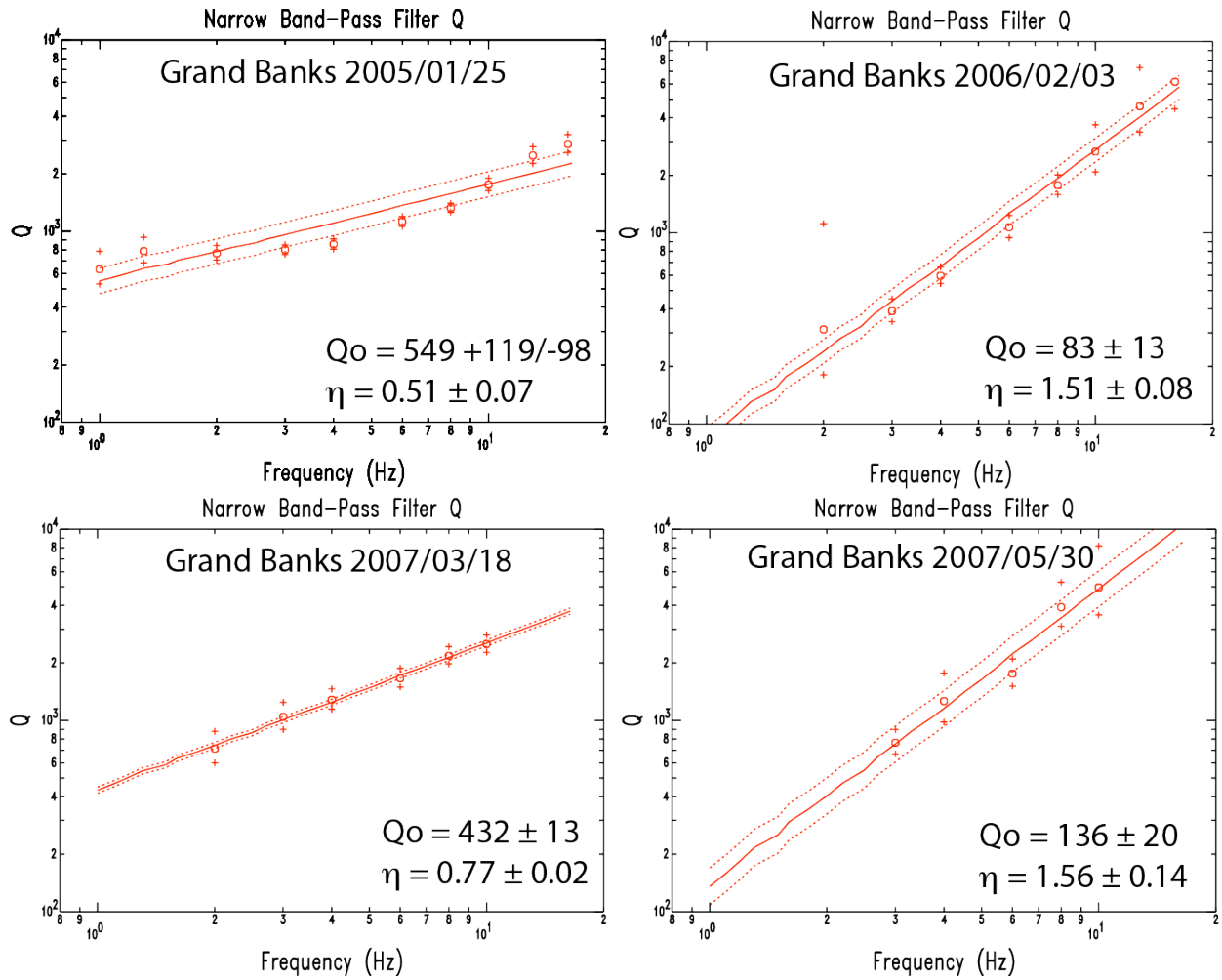


Figure 6: Plots of Q versus frequency for each earthquake in Table 2 and Figure 5. Mean Q at each frequency (octagons) and standard deviation (plus symbols above and below) are shown along with the mean fit (solid line) and 95% confidence levels for the mean fit (dotted lines) to Equation 3. Q_0 and η with their standard deviations for each earthquake are shown on each plot.

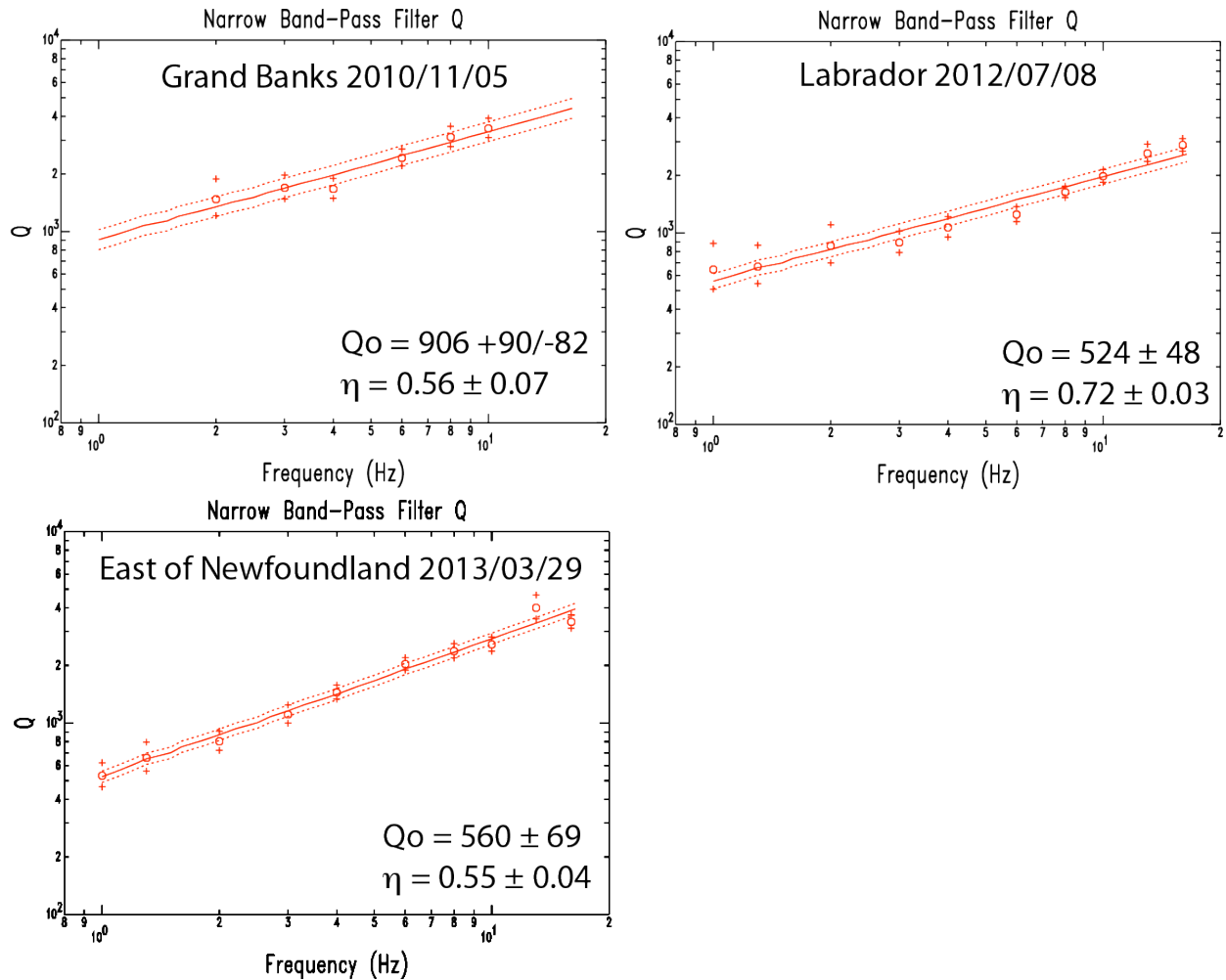


Figure 6 continued.

From the results in Figure 6 we can see that generally in easternmost Canada, Q_0 is 500 to 600 with η about 0.5 to 0.7, including the 2005 earthquake close to the epicenter of the 1929 Grand Banks earthquake and the 2013 earthquake east of Newfoundland (in submerged Appalachian crust – Lau et al., 2006). These values correspond well with the ENA midcontinent results of Atkinson and Boore (2014) of $Q_0 = 525 + 80/-70$ and $\eta = 0.45 \pm 0.033$ [uncertainties are standard deviations based on the individual frequency Q estimates in Figure 5 of Atkinson and Boore (2014) as provided by Gail Atkinson (written communication, October 26, 2013)].

The two earthquakes in the Laurentian Channel between Newfoundland and Nova Scotia show very low Q_s (Q_0 less than 200). This suggests a high attenuating region in this location. One event shows no Lg suggesting that it occurred in the upper mantle below the crust and the $Q(f)$ is for a mantle path. The other event does show Lg but still could have occurred close to the mantle in the crust. Depth control for the offshore earthquakes is not good due to a lack of offshore seismic stations. Seismic energy from earthquakes in other parts of easternmost Canada likely diffracts around this small region of low Q and hence this low Q region can not be seen in the Q results from these other events.

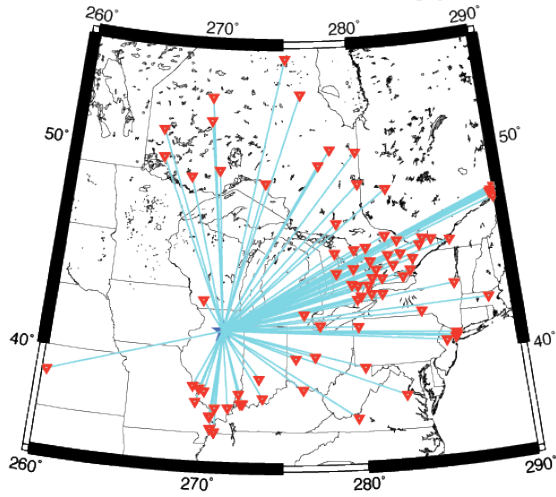
Q results for the two earthquakes in the Atlantic off the continental margin and further to the south and southeast from the 1929 Grand Banks event show a broader variation of Q_0 of 432 and 906 with similar η . This suggests a larger variation in Q about an ENA Q for Atlantic crust to the south and east of the continental margin, but would not effect the interpretation (see Cramer and Boyd, 2014) that the easternmost Canadian crust and continental margin is basically Appalachian Province with ENA Q. Mousavi et al. (2014), partly funded by this grant, analyzed Lg and Sn attenuation separately for this same region using 91 earthquakes and found $Q_{Lg} = 615 \pm 25 f^{0.35 \pm 0.04}$ and $Q_{Sn} = 404 \pm 23 f^{0.45 \pm 0.03}$. Our Qo results using both Lg and Sn, generally fall between the results of Mousavi et al. (2014), except for the farthest to the SE Atlantic and the two Laurentian Channel earthquakes. Mousavi et al. (2014) more clearly demonstrates that Q, and hence intensities, for raypaths from the 1929 Grand Banks M7.2 earthquake have ENA crustal values.

Continental US: The other focus of our regional Q investigation is the continental US, particularly those regions without estimates from other Q studies. Table 4 lists the earthquakes used in this portion of our study. Figures 7 and 8 present the results for selected regions in the continental US. The three major Q regions represented are the CEUS, Gulf Coast, and WUS. Figure 7 shows the raypaths for each earthquake from which Q(f) was estimated. Figure 8 shows the Q(f) results.

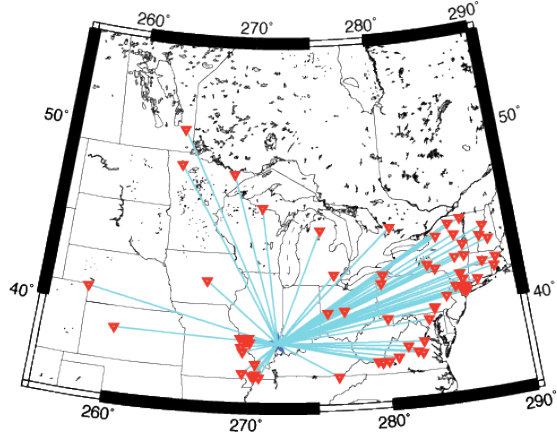
Table 4: Continental US earthquakes used in this study. Magnitudes listed are moment magnitudes. All earthquakes showed the presence of Lg in their records.

Prairie Center, IL 2004/06/28 M4.15
Mt. Carmel, IL 2008/04/18 M5.3
Slaughterville, OK 2010/10/13 M4.3
Sullivan, MO 2011/06/07 M3.9
Comal, TX 2011/10/20 M4.6
Nevada 2008/02/21 M5.9

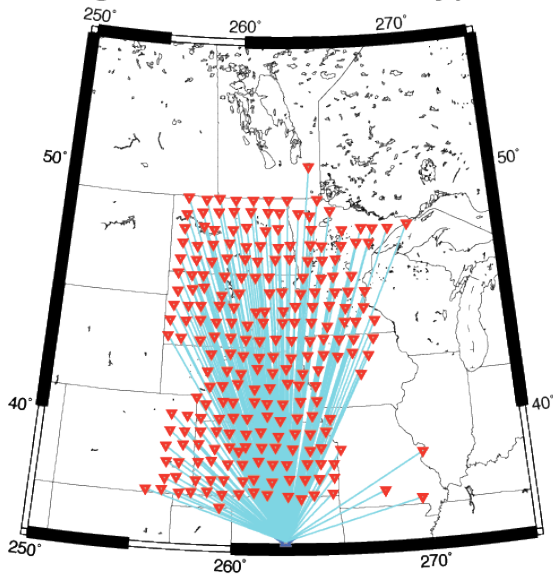
Prairie Cntr 2004 Raypaths



Mt Carmel M 2008 Raypaths



Slaughtervl N 2010 Raypaths



Sullivan 2011 Raypaths

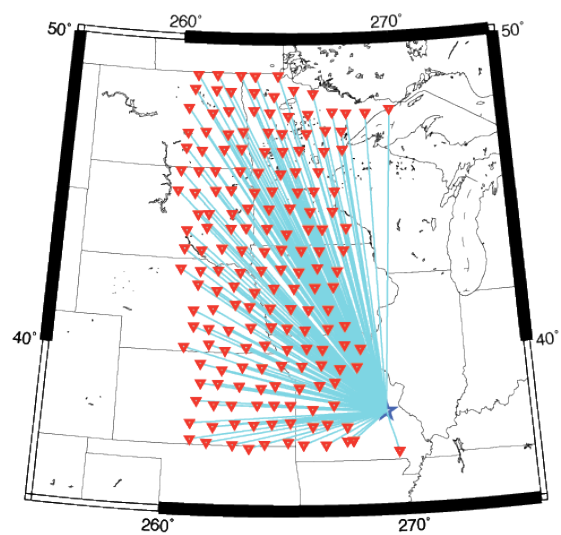
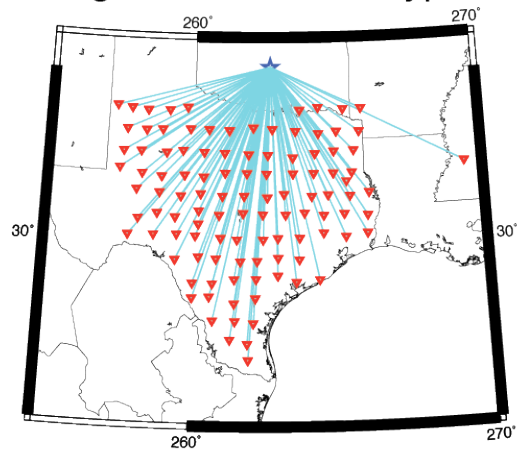
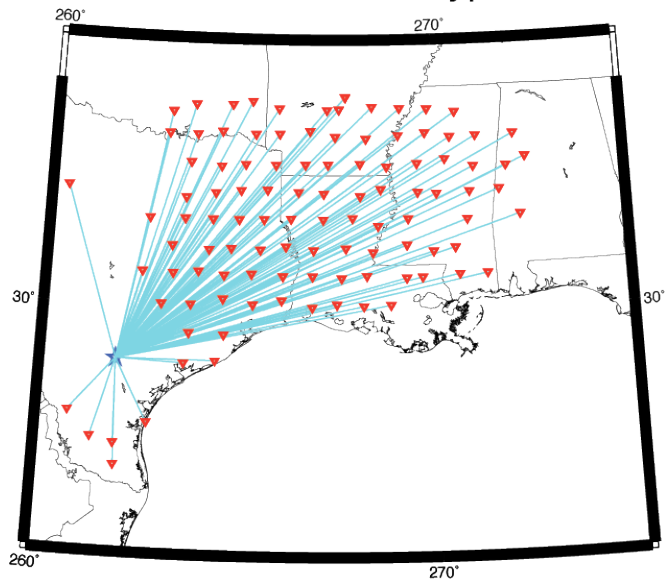


Figure 7: Continental US earthquake raypath maps for this study. Symbols and colors are the same as in Figure 5.

Slaughterville S 2010 Raypaths



Comal TX 2011 Raypaths



Nevada 2008 Raypaths

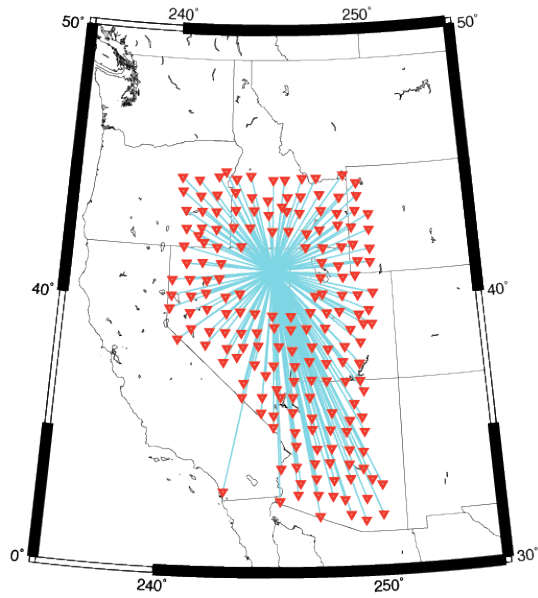


Figure 7 continued.

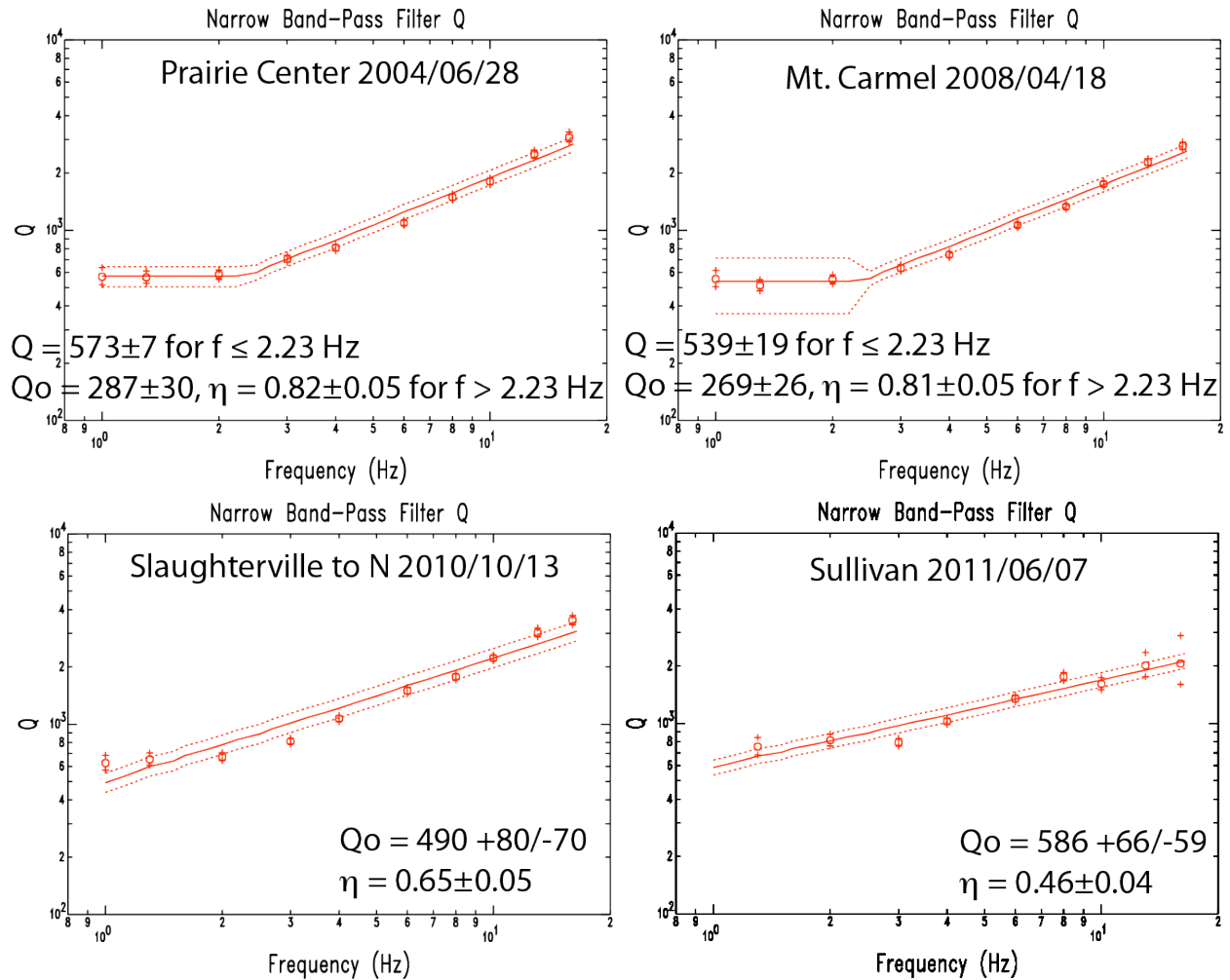


Figure 8: Plots of Q versus frequency for each earthquake in Table 3 and Figure 7. The presentation is the same as in Figure 6.

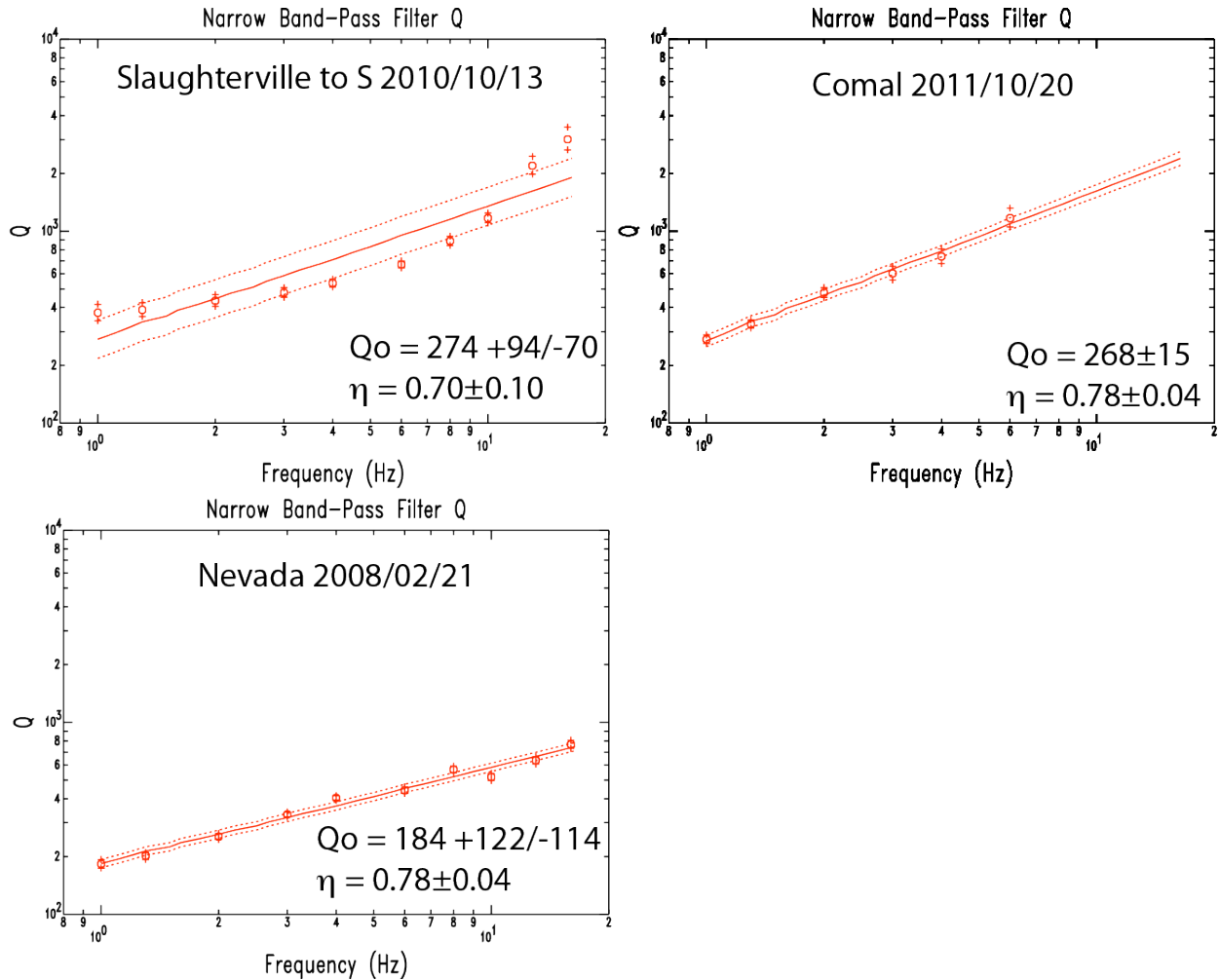


Figure 8 continued.

Figure 8 shows Q_0 estimates for the CEUS Midwest and Great Plains regions of 500 – 600, similar to Atkinson and Boore’s (2014) Q_0 of 525 for ENA. The older two CEUS earthquakes (Prairie Center and Mt. Carmel) predate the EarthScope USArray (TA) entry into the CEUS and have sparser station coverage and longer raypaths (up to 1700 to 1500 km, respectively). The Q versus frequency plots show distinctly constant Q for frequencies less than 2.5 Hz for the Midwest. The other two CEUS earthquakes (Slaughterville to the North and Sullivan) use observations from TA stations for the Great Plains covering distances up to 1600 and 1100 km, respectively. While the Slaughterville N and Sullivan Q versus frequency plots have a tendency toward constant Q below 2.5 Hz with Q values of 600 – 700 and 700 – 800, respectively, the constant Q trend is still within the uncertainty of the $Q(f)$ fit as shown in Figure 8. Thus we retain the $Q(f)$ fit for our initial estimation of Q in the crust under the Great Plains. However, this is an area for further research.

The two Q_0 estimates for the western Gulf Coast region in Figure 8 show values near 270. Estimates of η for this region are 0.70 – 0.80. Q_0 values for the western Gulf Coast are about half of the values for the CEUS region. As pointed out in Figure 4, the Gulf Coast region has distinct Q s from the CEUS. Our one regional Q estimate for the WUS is $Q_0 = 184 + 122/-114$

and $\eta = 0.78 \pm 0.04$. This Q estimate is similar to previous WUS Lg Q estimates such as Erickson et al., 2004 (see Table 4). Q_0 estimates for the WUS are at or below 200 and Gulf Coast estimates are closer to 300, with η in both regions being similar. This suggests that Q is different between the WUS, Gulf Coast, and CEUS as partially demonstrated in previous studies. This study demonstrates the distinctive Q for the Gulf Coast region versus the WUS and CEUS.

Table 4: Lg Q(f) values for the WUS from Erickson et al., 2004.

Northern California – $Q_0 = 152 \pm 37$, $\eta = 0.72 \pm 0.16$

Southern California – $Q_0 = 105 \pm 26$, $\eta = 0.67 \pm 0.16$

Basin and Range – $Q_0 = 200 \pm 40$, $\eta = 0.68 \pm 0.12$

Pacific Northwest – $Q_0 = 152 \pm 49$, $\eta = 0.76 \pm 0.18$

Rocky Mountains – $Q_0 = 166 \pm 37$, $\eta = 0.61 \pm 0.14$

Conclusions

The boundaries between major Q regions in the continental US are distinct and sharp at the 70 km grid spacing of the EarthScope USArray. The WUS-CEUS Q boundary seems more closely associated with the eastern front of the Rocky Mountains than at 110°W as used in the USGS National Seismic Hazard Maps (2008 and prior). The CEUS-Gulf Coast Q boundary seems to fall near 35°N in Arkansas and Oklahoma. Q_0 for the Gulf Coast is near 300 and is distinct from the WUS (less than 200) and CEUS (500 or greater). In easternmost Canada Q_0 is generally 500 to 600, similar to CEUS Q, although there may be a small region of low Q in the Laurentian Channel between Labrador and Nova Scotia that is difficult to detect (the low Q observations there may be due to the earthquakes occurring near or below the crust mantle boundary and not due to low crustal Q). The easternmost Canada Q results demonstrate that intensities from the 1929 Grand Banks earthquake are likely true ENA intensities and not different due to Q differences between the continent and the continental shelf in which the 1929 earthquake rupture occurred. Future work funded by another USGS NEHRP grant will further investigate CEUS and Gulf Coast Q east of the Mississippi River and develop a Gulf Coast empirical GMPE distinct from CEUS mid-continent GMPEs.

Acknowledgements

Figures in this report were generated using GMT (Wessel and Smith, 1991) and SAC (Goldstein et al., 2003).

References

Atkinson, G.M., and D.M. Boore (2013), The attenuation of Fourier amplitudes for rock sites in eastern North America, *Bull. Seism. Soc. Am.* **104**, 513-528.

Atkinson, G.M., and R.F. Mereu (1992), The shape of ground motion attenuation curves in southeast Canada, *Bull. Seism. Soc. Am.* **82**, 2014-2031.

Benz, H.M., A. Frankel, and D.M. Boore (1997), Regional Lg Attenuation for the Continental United States, *Bull. Seis. Soc. Am.* **87**, 606-619.

Claerbout, J. F. (1976), *Fundamentals of geophysical data processing with applications to petroleum prospecting*, McGraw-Hill, New York, NY, 274 pp.

Cramer, C.H. (2008), *Final Report on Initial Database Design for a Database of CEUS Ground Motions*, Final Technical Report to the USGS for first year of Cooperative Agreement 07CRAG0015, 26 pp.

Cramer, C.H., J. Kutliroff, and D. Dangkoa (2009), *Second Year Final Report on a Database of CEUS Ground Motions*, Final Technical Report to the USGS for Cooperative Agreement 07CRAG0015-Mod1, 12 pp.

Cramer, C.H., J.R. Kutliroff, and D.T. Dangkoa (2011), *Next Generation Attenuation East Initial Flat Files for Eastern North America*, Report to PEER accompanying NGA East flat files and time series under subagreement 7140, 4 pp.

Cramer, C.H., and O.S. Boyd (2014), Why the New Madrid earthquakes are M7-8 and the Charleston earthquake is ~M7, *Bull. Seis. Soc. Am.*, submitted.

Erickson, D, D.E. McNamara, H.M. Benz (2004), Frequency-Dependent Q within the Continental United States, *Bull. Seis. Soc. Am.* **94**, 1630-1643.

Faddeeva, V.N. (1959), *Computational Methods of Linear Algebra*, translated by C.D. Benster, Dover Publications, New York, p 90-99.

Goldstein, P., D. Dodge, M. Firpo, Lee Minner (2003), SAC2000: Signal processing and analysis tools for seismologists and engineers, Invited contribution to *The IASPEI International Handbook of Earthquake and Engineering Seismology*, Edited by WHK Lee, H. Kanamori, P.C. Jennings, and C. Kisslinger, Academic Press, London.

Lau, K.W.H., K.E. Loudon, T. Funck, B.E. Tucholke, W.S. Holbrook, J.R. Hopper, and H.C. Larsen (2006), Crustal structure across the Grand Banks – Newfoundland basin continental margin – I. results from a seismic refraction profile, *Geophys. J. Int.* **167**, 127-156.

Mousavi, S.M., C.A. Langston, and C.H. Cramer (2014), Lg blockage and attenuation of high-frequency regional phases within the continental margin of Nova Scotia, in preparation.

Phillips, W.S., and R.J. Stead (2008), Attenuation of Lg in western US using USArray, *Geoph. Res. Ltrrs.* **35**, L07307, DOI: 10.1029/2007/GRL032926.

Wessel, P. and W. H. F. Smith (1991). Free software helps map and display data, *EOS Trans. AGU* **72**, 441.

Publications from this Research

Although one paper (Mousavi et al., 2014) is in preparation, no publications have resulted from this research as of this date. Future papers based on this work will be provided, as required, when publication occurs.